Spray characterization of pneumatic concentric nebulizer used in Inductively Coupled Plasma – Mass Spectrometry (ICP-MS)

A. Kashani*, D. Bandura, J. Mostaghimi

Department of Mechanical and Industrial Engineering, University of Toronto, 5 Kings College Road, Toronto, Ontario, M5S 3G8, Canada

Abstract

A Type-C glass concentric pneumatic nebulizer, widely used for sample introduction in MS, is characterized. This class of nebulizer disintegrates a pre-filmed liquid sample by the aid of a highly compressible co-flowing gas stream whose velocity is order of magnitudes larger than that of the liquid. Although the ICP-MS nebulizers generally follow the fundamentals of pneumatic atomization, they require separate characterization due to their specific design, dimension, geometry and different flow parameters typical for the ICP-MS operating conditions. For instance, employing the Nukiyama-Tanasawa (NT) [1] and the Rizk-Lefbvre (RL) [2] models, to the ICP-MS nebulizers for size prediction leads to erroneous results. Nevertheless RL model is modified to improve the agreement with experiment. The theoretical unseeded axial gas velocity is compared to the measured mean velocity of the sprayed droplets where shown, the difference is larger at lower gas flow rates. The results of size and velocity characterization are then used to study nebulizer performance at different flow conditions and are then fed into a Maximum Entropy Principle (MEP) model to predict aerosol size and velocity distribution. In the present task, a new point-wise MEP-based model is implemented.

Introduction

Modeling spray size and velocity distribution is of significant importance in many industrial applications ranging from coating, agriculture, pharmaceutical processes, combustion engines, sample introduction in ICP-MS, etc. since drops size and velocity directly determine the overall performance of such systems. For instance, in MS droplets below *10 μm* traveling at a particular range of velocities are highly desired and guarantees complete droplet desolvation, evaporation, atomization and ionization in plasma [3]. Therefore from practical point view, it would be crucial to know what fraction of the atomized droplets can meet the requirements of an efficient mass spectrometry.

As the stochastic nature of the spray systems has drastically limited the development of mathematical modeling, a number of empirical correlations are proposed for this purpose, for instance Rosin-Rammler [4], Nukiyama-Tanasawa [5] and log-normal [6]. Nevertheless, they do not necessarily offer universal prediction, if not employed in the range they have been proposed and tested; besides these correlations are not founded on a mathematical ground and could be considered more or less as curve-fitting models that are only applicable to a certain range of experiments.

The maximum entropy principle is currently one of the promising mathematical approaches for prediction of spray size and velocity distribution. The principle seeks the least biased distribution based on the limited available pieces of information regarding the spray distribution and is capable of modeling a wide range of practical problems. In this task a new point-wise MEP-based model will be implemented.

Experiment

A Type-C CN [7] with capillary diameter of *260 μm* and a recessed tip of *500 μm* was connected to a supply of argon. The flow of argon was varied from *200-800 sccm* and controlled by a readout and mass flow controller (MKS, Type246C, MKS Instrument, MA, USA). Distilled water and methanol were used as liquid samples and were

Corresponding Author: Arash Kashani, akashani@mie.utoronto.ca

injected at *1*, *5* and *10 μl/s* through a 1cc-glass (Hamilton Company, MS, USA) syringe and the liquid flow rate was controlled by a model-22 syringe pump (Harvard apparatus, MS, USA). A two-component PDPA device (TSI Inc, MN, USA) recorded droplet size and velocity with a minimum measurable size of *0.5 μm*. The transmitter and receiver probes of the PDPA system were placed at *30* degree scattering angle and the measurements were taken *10 mm* downstream of the nebulizer tip to avoid high rejection rates of droplets and interference of the laser beams with the experiment setup. An image of the CN is presented in Figure 1.

Droplet size characterization and Atomization efficiency

Nukiyama-Tanasawa equation is the most commonly used model for size prediction of pneumatic atomizers since 1938 [1]. In this relation (equation 1) D_{32}, σ,V,ρ_l,η_l, Q_l and Q_g are Sauter mean diameter (μm), surface tension (*dynes/cm*), the relative velocity between the gas and liquid at the nebulizer exit (*m/s*), liquid density (g/cm^3), liquid viscosity (*poise*), liquid and gas flow rates (*l/min*) respectively. The equation is composed of a viscous and a non-viscous term and is defined for $0.8< \rho_l <1.2$, $30<\sigma<73$ and $0.01<\eta_l<0.8$ to characterize a jet-injection nebulizer. In Nukiyama-Tanasawa's experiment (NT model) the nozzle dimensions had little effect on the D_{32} value; therefore geometrical parameters are excluded in this correlation.

$$D_{32})_{NT} = \frac{585}{V}\left(\frac{\sigma}{\rho_l}\right)^{0.5} + 597\left(\frac{\eta_l}{\sqrt{\sigma\rho_l}}\right)^{0.45}\left(\frac{1000Q_l}{Q_g}\right)^{1.5} \qquad (1)$$

Here, the gas velocity at the nebulizer exit is estimated from the ideal gas law and the isentropic [8] theory. The theory provides good engineering estimation of the gas exit velocity for equation (1) and not necessarily its exact value.

As will be discussed in the result section, the Nukiyama-Tanasawa equation (1), largely overestimates the predicted value for Sauter mean diameter. Lefebvre [10] also derived a general correlation for the drop size of mechanical airblast atomizers as follows:

$$D_{32})_{RL} = Ad_o\left(\frac{\sigma}{\rho_g V^2 d_o}\right)^a\left(1+\frac{Q_l\rho_l}{Q_g\rho_g}\right)^b + Bd_o\left(\frac{\eta_l^2}{\sigma\rho_l d_o}\right)^c\left(1+\frac{Q_l\rho_l}{Q_g\rho_g}\right) \qquad (3)$$

Where coefficients are $a=0.5$, $b=1$ and $c=0.5$. In contrast to the NT model, Lefebvre's correlation can be presented in non-dimensionalized form whereas the effect of nozzle dimension (d_0) is included.

Rizk-Lefebvre [2] (RL model), tailored this equation for a specific airblast atomizer. By considering some secondary factors, they suggested the following coefficients: $A=0.48$, $a=0.4$, $b=0.4$, $B=0.5$ and $c=0.5$. Kahen et al. [9] reported an underestimation when the RL model was applied to microconenteric nebulizers, thus they modified the RL model through the coefficients, in a similar approach as [11], $A=0.54$, $a=0.31$, $b=0.5$, $B=0.16$ and $c=0.48$. We have similarly optimized the RL model for the CN, however coefficients A and B were kept as in reference [11] and $c=0.5$ was left untouched as in the original RL model [2] because for low-viscosity fluids the second term is of less significance. The results of NT, original and modified RL models for the CN's under ICP-MS nominal operating conditions are discussed later.

The role of an atomizer is to convert kinetic energy to surface energy in order to promote heat and mass transfer. Therefore, Atomization efficiency defined as the spray surface energy per unit time to the initial kinetic energy of the liquid can be expressed by equation (4). The efficiency of the CN is presented in the Results section.

$$efficiency = \frac{SE}{KE} = \frac{\dot{n}\,{}^{\pi}/_{4}\,\sigma\sum n_i D_i^2}{{}^{1}/_{2}\,\dot{m}_l\,U_{cap}^2} = \frac{\sigma\dot{n}\left({}^{\pi}/_{4}\right)\left(\sum n_i D_i^2\right)}{\underbrace{{}^{1}/_{2}\,\rho_l U_{cap}^2}_{\propto \Delta P_g}\,\dot{n}\left({}^{\pi}/_{6}\right)\left(\sum n_i D_i^3\right)} = \frac{6\sigma}{D_{32}\Delta P_g} \qquad (4)$$

Once D_{32} is known from the optimized model (equation 3), the atomization efficiency is calculated easily by having the sample surface tension and the applied pressure difference across the nebulizer.

Droplet velocity characterization

In MS the carrier gas atoms and droplets must have sufficient residence time in the central channel of ICP, hence both gas and droplet velocities have to be adequate and controlled, besides droplets with large ranges of size and velocities produce emission and mass spectrometric signals at different locations in the plasma which leads to reduced sensitivity and signal fluctuation [12]. Therefore ICP-MS prediction of the droplet velocity is of the same importance as the droplet size. Here, we are interested only in size and velocity of the droplets travelling along the centerline of the nebulizer since these droplets are most likely the ones that reach the plasma channel [9] and will not be lost due to dispersion in the delivery tube. The gas exit velocity can be calculated from the isentropic theory. For pneumatic nebulizers, a potential core exist which extends about seven times the jet diameter downstream where the exit velocity is conserved. From this point on, the axial velocity drops exponentially [13] as follows:

$$\frac{u_g(x)}{u_g(x=0)} = \frac{Kd_0}{x} \qquad (5)$$

here $u_g(x)$ is the desired axial velocity. A K value of *6.4* has been proposed by Tennekes and Lumley [14] for pneumatic nebulizers.

Maximum Entropy Principle

The conventional deterministic methods fail miserably in predicting spray size and velocity probability distribution functions (pdf) [15]. As MEP states while there are infinite ways to distribute droplets in the size and velocity space, the least biased distribution for a given set of constraints, is the one that maximizes the Shannon entropy [16]. The employed constraints for this study are normalization, mass, momentum, kinetic and surface energies and partition of surface energy. The mathematical derivation and the implemented constraints are not presented here but may be found in [17]. The joint size and velocity pdf that satisfies entropy maximization is given below.

pdf: $$f = \exp\left(-a_0 - a_1\overline{D}^2 - a_2\overline{D}^3 - a_3\overline{D}^3\overline{U} - a_4\overline{D}^3\overline{U}^2 - a_5\overline{D}^{-1}\right) \qquad (6)$$

Coefficients a_0-a_5 must be found numerically as in [17]. It should be noted that in this formulation size is normalized by D_{30} while velocity normalization was done by a reference velocity. Mitra and Li [15] and Sellens [17] applied MEP to the entire spray cross section thus they were limited to use liquid velocity at the nozzle exit and the sheet velocity for normalization respectively. However the MEP may also be applied locally (point-wise) if the local constraints are known. Since we are interested in the fate of the drops travelling along the centre line, MEP must be employed point-wise. We have used the local predicted gas velocity (equation 5) for normalization which is also a good measure of drop velocities of the spray.

Results

Figure (2) shows the predicted results of NT, RL, and the present optimization of RL model for a representative case of Q_l=*5 µl/s* at different gas flow rates. As can be seen the NT and RL model correctly predict the trend while D_{32} is significantly overestimated from the NT model whereas the original RL model shows considerable underestimation. The present optimized RL model shows reasonable agreement with experiment. The same trend was also observed for Q_l=*1* and *10 µl/s*, although the results are not included here. We may conclude from these results that the correlations used for typical pneumatic nozzles of [1] and [2] cannot be generalized to ICP-MS nebulizers without modification due to differences in dimensions, flow regimes, etc. For instance, the NT equation (1) has been developed for nozzles working well below sonic conditions, while most ICP-MS pneumatic nebulizers operate close to sonic conditions, besides the liquid uptake rate of ICP-MS nebulizers are not comparable to those presented in [1][2].

Figures (3) and (4) depict variation of two characteristic diameter ratios (required for MEP modeling). Here both the D_{30}/D_{32} and D_{30}/D_{-10} ratios are almost independent of liquid flow rates and are highly influenced by the gas flow rate. By increasing the gas flow rate, D_{30}/D_{32} ratio increases while D_{30}/D_{-10} decreases gradually. These trends suggest that the spray becomes narrower at higher gas flow rates which is probably due to the fact that at higher gas

flows, drops can better maintain the momentum gained in the potential core of the gas jet and avoid dispersion, thus more uniform drop sizes pass the probe volume. The size and velocity distribution graphs confirm this statement.

The atomization efficiency curves versus gas flow rate are presented in Figure (5). As can be seen, efficiency drops by increasing the gas flow rate and converges toward a same value for all the curves at high gas flows as it is theoretically impossible to convert all the initial kinetic energy to surface energy.

The difference between the measured mean droplet velocity and the predicted axial velocity (at $x=10\ mm$) decreases from *80%* to about *6-8%* by increasing the gas flow rate in Figure (6) which implies the momentum transfer between the two phases is smaller at higher gas flow rates therefore the unseeded gas velocity and mean drop velocities are comparable. The figure also shows the predicted axial velocity reaches a plateau, however the mean velocities continue to increase, i.e. the sonic conditions is delayed to higher gas flow rates or back pressure as reported in [8]. The ratio of root mean squared to mean velocity is presented in Figure (7). The figure clearly shows the ratio drops by increasing the gas flow rate and also verifies the previous finding regarding the gradual decrease of distribution span at higher gas flows.

Figures (8-9) presents the prediction of MEP modeling for size and cumulative size distributions, for the sample case of $Q_g=500\ sccm$ and $Q_l=5\ \mu l/s$ at $x=10\ mm$. As can be seen the agreement is reasonable. For instance, the model covers the span of distribution correctly, although a difference between the peaks of two distributions is observed. The cumulative graph shows *70* percent of droplets are below the $D_{10}/D_{30}=0.79$ and the percentage drops is *35* percent for $D/D_{30}=0.62$ a number corresponding to $10\ \mu m$ droplets consumable for plasma.

The velocity distribution graphs of Figures (10-11) show the most probable velocity is smaller than the predicted gas velocity. For instance while, *40* percent of drops are below the peak velocity, *75* percent of them have velocities below the gas velocity. At $U/u_g>0.7$, the error between the experiment and coupled MEP models grows considerably, besides the end tails' population of the pdf do not match with the experiment (Figure 10) and the peak velocity shows some difference. This issue can also be observed in Mitra and Li's study [15] and some other literature and has not been addressed yet. The form of the joint pdf (equation 6) probably caused the issue, since for example a simple Gaussian pdf of mere velocity (green line in Figures 10-11) shows better agreement with experiment whilst maximizes the entropy function. However, it should be noted that the presented pdf's are mathematically correct and are the least biased and the most objective results for the selected form of the pdf (equation 6) as far as maximization of the entropy is concerned. The fact that the presented pdf shows some unphysical behavior may suggest that either different form of information must be specified or additional constraints should be applied as stated by Kapur [18]. Further study is required to resolve this issue.

Conclusion

The typical dimension, geometry and flow parameters of the ICP-MS nebulizers distinguish them from the mechanical engineering nozzles specifically those in [1]-[2]. Thus, for instance the widely used NT and RL model cannot be employed for size characterization. The RL model however was optimized to characterize a Type-C CN. The predicted gas velocity from the isentropic theory shows good agreement with drop mean velocities at high gas flow rates; where the rate of momentum transfer from gas to liquid is small. The atomization efficiency at high gas flow rates becomes almost independent of the volume rate of the sprayed liquid. The results of size and velocity characterization were fed as input to a coupled MEP model. The reasonable agreement was observed for the size distribution while the velocity distribution shows some unphysical behavior that has not been addressed yet. The results however are the most objective and least biased representation for the given form of the pdf and the input constraints. Further investigation is required in order to have a mathematically and physically correct spray model.

References

[1] Nukiyama S., Tanasawa Y., Transactions of the Japan society of mechanical engineers, 4-6, reports 1-6., 1938-40.
[2] Rizk N.K., Lefebvre A.H., Journal of engineering for gas turbines and power, 106, pp. 634-638, 1984.
[3] Montaser A., Golightly D.W., "Inductivley coupled plasma in analytical atomic spectrometry", 2nd edition, p. 238, 1992.
[4] Rosin P., Rammler E., Journal of institute of fuel, 7, pp. 29-36, 1933.

[5] Nukiyama S., Tanasawa Y., Transl Hope E., Defense research board, Department of national deffence, Ottawa, Ontario, Canada.
[6] Crown E.L., "Lognormal distributions: theory and applications", New York, Marcel Dekker, 1988.
[7] www.meinhard.com
[8] Sharp B.L., Journal of analytical atomic spectrometry, 3, pp. 613-652, 1988.
[9] Kahen K, Acon B.W., Montaser A., Journal of analytical atomic spectrometry, 5, pp/ 631-637, 2005.
[10] Lefebvre H., Progress in energy and combustion science, 6, pp. 233-261, 1980.
[11] Gras L., Mariela L, Canals A., Journal of analytical atomic spectrometry, 17, pp. 524-529, 2002.
[12] Olesik J.W., Smith E.J., Williamsen E.J., Journal of analytical chemistry, 61, pp. 2002-2008, 1989.
[13] Sharp B.L., Journal of analytical atomic spectrometry, 3, pp. 939-963, 1988.
[14] Tennekes H., Lumley J.L., "A first course in turbulence", MIT Press, MA, 1972.
[15] Mitra S.K., Li X., Energy conversion engineering conference, 2, pp. 904-909, 1997.
[16] Shannon C.E., Bell systems technical journal, 27, pp. 379-423, 623-656, 1948.
[17] Sellens R.W., Particle and particle system characterization, 6, pp. 17-27, 1989.
[18] Kapur J.N., Journal of mathematical and physical sciences, pp 103-156, 1983.

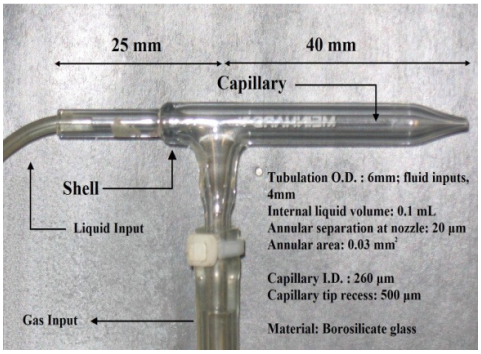

Figure 1- Type-C CN.

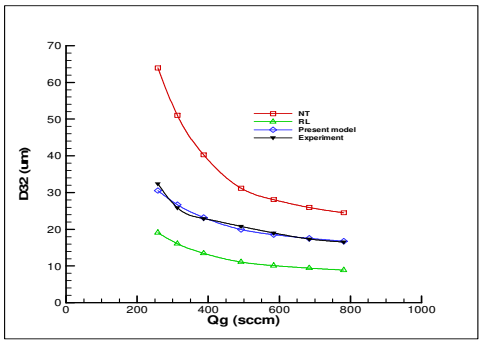

Figure 2- D_{32} vs. Q_g for Q_l=5 $\mu l/s$ flow rate, liquid: distilled water

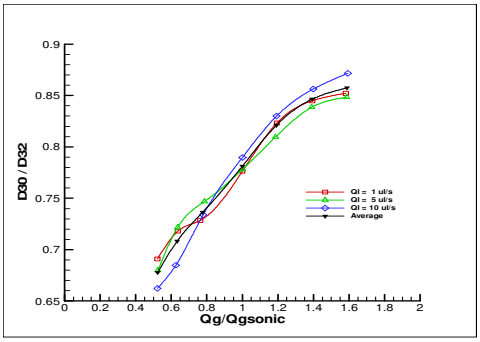

Figure 3- D_{30}/D_{32} ratio vs. Q_g at different liquid flow rates, liquid: distilled water

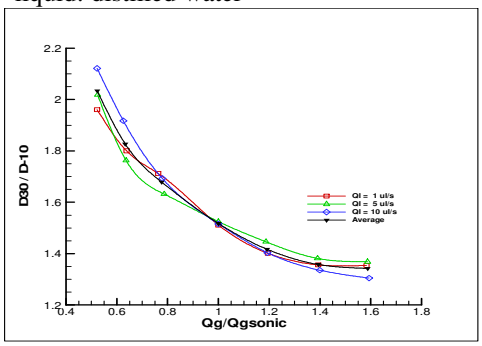

Figure 4- D_{30}/D_{-10} ratio vs. Q_g at different liquid flow rates, liquid: distilled water

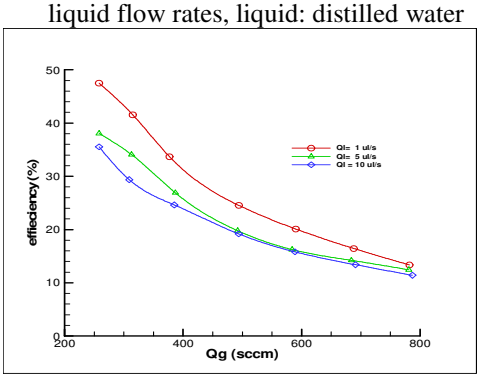

Figure 5- Atomization efficiency vs. Q_g at different liquid flow rates, liquid: distilled water

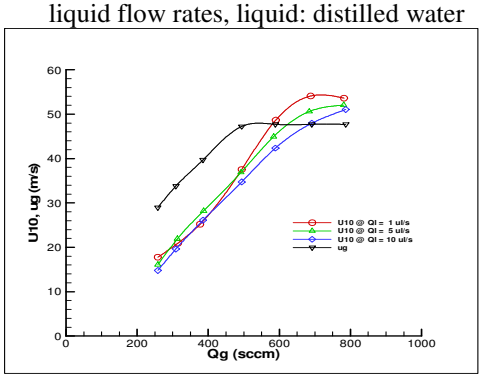

Figure 6- U_{10} and u_g vs. Q_g at different liquid flow rates, liquid: distilled water

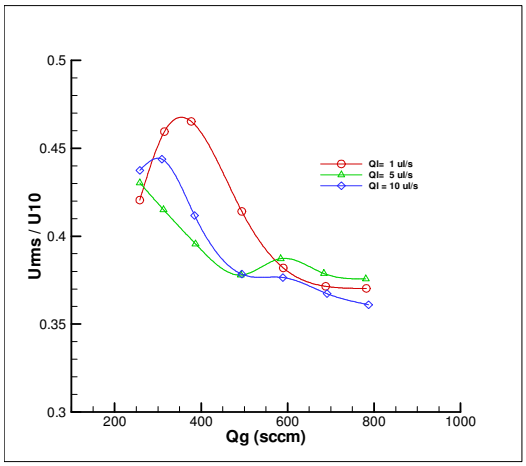

Figure 7- U_{rms}/U_{10} ratio vs. Q_g at different liquid flow rates, liquid: distilled water

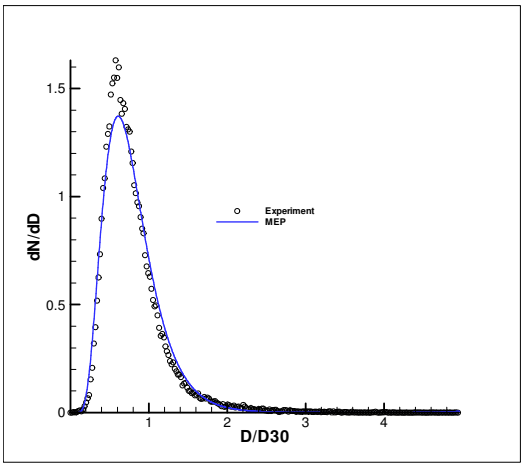

Figure 8- size distribution at Q_l=5 *µl/s* and Q_g=*500 sccm*, liquid: distilled water

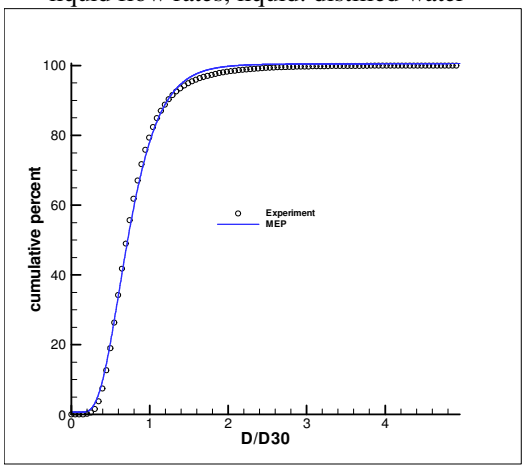

Figure 9- cumulative size distribution at Q_l=5 *µl/s* and Q_g=*500 sccm*, liquid: distilled water

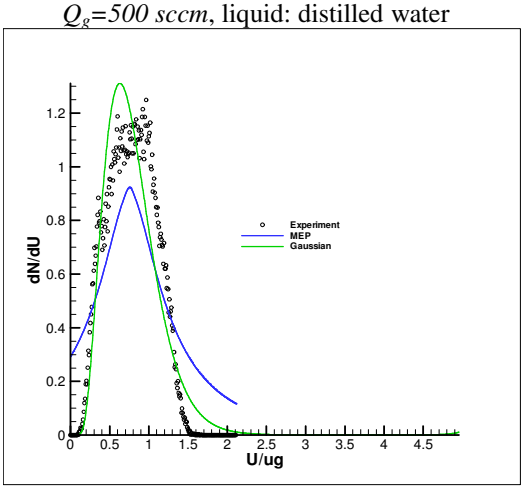

Figure 10- velocity distribution at Q_l=5 *µl/s* and Q_g=*500 sccm*, liquid: distilled water

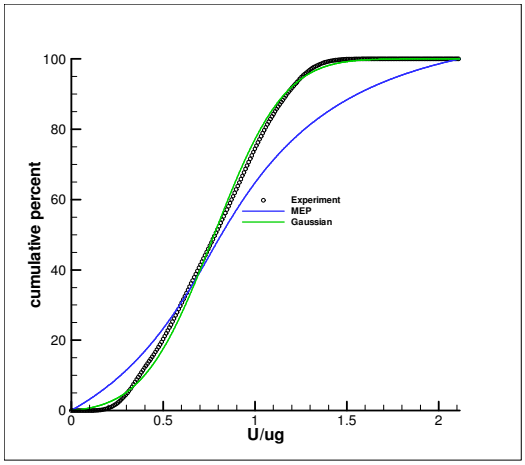

Figure 11- cumulative velocity distribution at Q_l=5 *µl/s* and Q_g=*500 sccm*, liquid: distilled water